

Totally asymmetric simple exclusion process on multiplex networks

Cite as: Chaos **30**, 023103 (2020); <https://doi.org/10.1063/1.5135618>

Submitted: 07 November 2019 . Accepted: 13 January 2020 . Published Online: 03 February 2020

Guojiang Shen, Xinye Fan , and Zhongyuan Ruan 

COLLECTIONS

 This paper was selected as an Editor's Pick



View Online



Export Citation



CrossMark

ARTICLES YOU MAY BE INTERESTED IN

[Characterizing the complexity of time series networks of dynamical systems: A simplicial approach](#)

Chaos: An Interdisciplinary Journal of Nonlinear Science **30**, 013109 (2020); <https://doi.org/10.1063/1.5100362>

[Merger of a Hénon-like attractor with a Hénon-like repeller in a model of vortex dynamics](#)

Chaos: An Interdisciplinary Journal of Nonlinear Science **30**, 011105 (2020); <https://doi.org/10.1063/1.5144144>

[How entropic regression beats the outliers problem in nonlinear system identification](#)

Chaos: An Interdisciplinary Journal of Nonlinear Science **30**, 013107 (2020); <https://doi.org/10.1063/1.5133386>

Scilight Highlights of the best new research
in the **physical sciences**

[LEARN MORE!](#)



Totally asymmetric simple exclusion process on multiplex networks

Cite as: Chaos 30, 023103 (2020); doi: 10.1063/1.5135618

Submitted: 7 November 2019 · Accepted: 13 January 2020 ·

Published Online: 3 February 2020



View Online



Export Citation



CrossMark

Guojiang Shen,¹ Xinye Fan,¹  and Zhongyuan Ruan^{1,2,a)} 

AFFILIATIONS

¹College of Computer Science, Zhejiang University of Technology, Hangzhou 310023, China

²Institute of Cyberspace Security, Zhejiang University of Technology, Hangzhou 310023, China

^{a)}Author to whom correspondence should be addressed: zyruan@zjut.edu.cn

ABSTRACT

We study the totally asymmetric simple exclusion process on multiplex networks, which consist of a fixed set of vertices (junctions) connected by different types of links (segments). In particular, we assume that there are two types of segments corresponding to two different values of hopping rate of particles (larger hopping rate indicates particles move with higher speed on the segments). By simple mean-field analysis and extensive simulations, we find that, at the intermediate values of particle density, the global current (a quantity that is related to the number of hops per unit time) drops and then rises slightly as the fraction of low-speed segments increases. The rise in the global current is a counterintuitive phenomenon that cannot be observed in high or low particle density regions. The reason lies in the bimodal distribution of segment densities, which is caused by the high-speed segments.

Published under license by AIP Publishing. <https://doi.org/10.1063/1.5135618>

The totally asymmetric simple exclusion process (TASEP) is a paradigmatic model for describing the one-dimensional transport in which the excluded-volume effect of entities (or “particles”) is taken into account. This model and its extensions have been studied extensively in the context of one-dimensional lattices or simple (one-layer) networks. However, many real systems, such as social relational networks or transportation networks, exhibit more complex structures—they are intrinsically multi-layer. In this paper, we try to understand how the multiplex networks may influence the TASEP. We find a counterintuitive phenomenon when considering the TASEP on multiplex networks: in some circumstances, lowering the traveling speed of particles on a fraction of links may result in a better performance in the global traffic flow. This paradox is quite different from the classical Braess paradox, since in our model, the particles travel totally at random. Our results may provide some deep insights for transportation authorities to cope with traffic jams in reality.

I. INTRODUCTION

Transport phenomena, like water transport in plants, vehicle motion in road networks,^{1–3} or human mobility in different geographic regions,^{4–7} have been well studied by researchers from

various disciplines. The totally asymmetric simple exclusion process (TASEP), which takes into account the excluded-volume effect of entities (meaning that they cannot occupy the same place at the same time), is a paradigmatic model to describe the transport of particles in one-dimensional lattices (or chains).^{8,9} This model was first raised by MacDonald, used for studying the kinetics of RNA polymerization by ribosomes.^{10,11} In TASEP, the particles hop in a given direction along a one-dimensional chain, which consists of a number of inner sites based on the following rule: a particle can hop one step forward only if the neighbor site is unoccupied. Though the model is simple, it can yield abundant dynamics. Under different conditions, there may appear three different homogeneous phases (namely, high density, low density, and maximal current) or a non-homogeneous shock phase in which low density and high density regions coexist.⁸

The TASEP model and its related variants have been explored extensively, with most of the studies focusing on one-dimensional transport.^{12–19} Neri *et al.* first investigated TASEP on networks.¹¹ In their model, particles on the links (segments) move according to the normal TASEP rule, while at the junctions (vertices), they choose one of the outgoing segments at random. Based on simple mean-field analysis, they demonstrated that TASEP on a random Bethe network can lead to a plateaulike region in the current–density diagram. While for Poissonian networks, the randomness in the

vertex degrees can greatly modify the transport features. After this seminal work, much attention have been paid to the study of the TASEP on simple networks. For example, Baek *et al.* improved the mean-field theory by considering the correlations at junctions and found some notable deviations from the classical results.²⁰ Motishaw *et al.* investigated the TASEP on a tree network where the aggregate hopping rate is constant and showed that the phase diagram is the same as that in the one dimensional case.²¹ Recently, Bitihn and Schadschneider studied the Braess paradox in the transport network of TASEP.²²

These studies all assume that the underlying networks are single-layered (or isolated). However, many real systems are composed of several layers of networks, exhibiting multilayer (or multiplex) properties.^{23–26} For instance, the air transportation network where nodes stand for airports and links represent direct flights between two airports is multiplex if one considers that different commercial airlines may be operated by different companies.²⁷ Another typical example is the road traffic network composed of high-speed railways and highways, where the traveling speeds vary significantly.²⁸ Studying different dynamical processes (such as epidemic spreading, information cascades, etc.^{29,30}) on multilayer networks has gained much attention recently.^{31–33} Nevertheless, our understanding of TASEP on multilayer networks is very limited. This problem is of significant importance in some areas like urban transportation, where how the complex (multilayer) road network may affect the traffic flow is still not quite clear.

In this paper, we study the TASEP model on multiplex networks where the segments are classified into two types—high-speed segments and low-speed segments. Our analytical and simulation results show that the multiplex structure (or heterogeneity in segments) affects the global traffic flow in a nontrivial way. Specifically, the global current, which is defined as the number of hops per unit time divided by the total number of sites, may drop as the fraction of high-speed segments increases under certain circumstances.

The paper is organized as follows. In Sec. II, we present the details of our model. In Sec. III, we perform a simple mean-field analysis of our model. In Sec. IV, we consider the TASEP on single-layer networks. In Sec. V, we study the TASEP on multiplex networks. Finally, we make a conclusion in Sec. VI.

II. MODEL

Let us start by considering a directed random regular network of N vertices (or junctions) and E links (or segments). Each vertex has c outgoing links and c incoming links, which are connected randomly to other vertices. Each link, $i \rightarrow j$ (where $i, j \in V$ and V is the set of vertices), consists of L inner sites. Thus, the total number of sites (including the vertices) is $N_s = N(cL + 1)$. Suppose there are M particles distributed in the network, where each site can only hold utmost a single particle. The global particle density, thus, is $\rho = M/N_s$. According to TASEP, we assume the hops of particles obey the following rules:

(1) If a particle is occupying an inner site of a link (e.g., $u \rightarrow v$) whose neighbor site in the link direction is vacant, it will move from the current site to the neighbor one with probability p_{uv} , while if the neighbor site is occupied, the particle will stay still.

(2) If a particle is occupying a vertex, it will choose one of the outgoing links at random as the next moving direction. If the first inner site of the chosen link (e.g., $v \rightarrow w$) is vacant, the particle will move to this site with probability p_{vw} ; otherwise, it will stay at the vertex.

We update the sites asynchronously. In each time step $\Delta t = 1/N_s$, a site is randomly chosen to be updated so that every site is updated once per unit time on average. We define the global current J as the average number of hops per unit time per site.

The links in the system are classified into k different types, with each type corresponding to a certain value of hopping probability. For simplicity, we let $k = 2$ in this paper, i.e., there are two types of links that form a two-layer (multiplex) network (as shown in Fig. 1). Note that the vertices in both layers are the same. On the first layer (say, layer A), every particle moves with probability p_A at each time step if its neighbor site in the link direction is vacant. Without loss of generality, we set $p_A = 1$. On the second layer (say, layer B), the particles hop with probability p_B which is smaller than p_A , meaning that the particles move more slowly. In our model, we randomly choose a fraction r of links as low-speed ones, on which the particles hop with probability $p_B < 1$. Clearly, if $r = 0$, it returns back to the previous model studied in Ref. 11.

III. MEAN-FIELD ANALYSIS

We first consider the situation of an isolated segment with entry rate α , exit rate β , and hopping rate p . The number of the inner sites is L . Neglecting the boundary effects, the average density ρ_{seg} (or bulk density) of the segment and the current J_{seg} can be computed as follows (both are functions of p , α , and β):^{8,34}

$$\rho_{seg}(p, \alpha, \beta) = \begin{cases} \frac{\alpha}{p}, & \alpha < \frac{p}{2}, \alpha \leq \beta \text{ (LD)}, \\ 1 - \frac{\beta}{p}, & \beta < \frac{p}{2}, \alpha \geq \beta \text{ (HD)}, \\ \frac{1}{2}, & \alpha, \beta \geq \frac{p}{2} \text{ (MC)}, \end{cases} \quad (1)$$

and

$$J_{seg}(p, \alpha, \beta) = p\rho_{seg}(p, \alpha, \beta)(1 - \rho_{seg}(p, \alpha, \beta)). \quad (2)$$

There are three homogeneous phases in the system: high density (HD), low density (LD), and maximal current (MC). While for $\alpha = \beta$, there arises another nonhomogeneous phase—shock phase, in which the high and low density phases coexist, separated by a domain wall whose position can fluctuate on the segment.

In networks, the vertices play a crucial role in the transportation process. The particles from different segments will compete to occupy the same vertex which may significantly constrain the traffic flow. Let $\rho_v(t)$ be the average occupancy of vertex v at time t . The conservation of the number of particles at vertex v implies that

$$\frac{\partial \rho_v}{\partial t} = \sum_{u \rightarrow v} J_{uv} - \sum_{w \leftarrow v} J_{vw}, \quad (3)$$

where J_{uv} is the current on the segment $u \rightarrow v$, the sum $\sum_{u \rightarrow v}$ runs over vertices u that point to the vertex v , and the sum $\sum_{w \leftarrow v}$ runs over vertices w that are pointed by the vertex v .

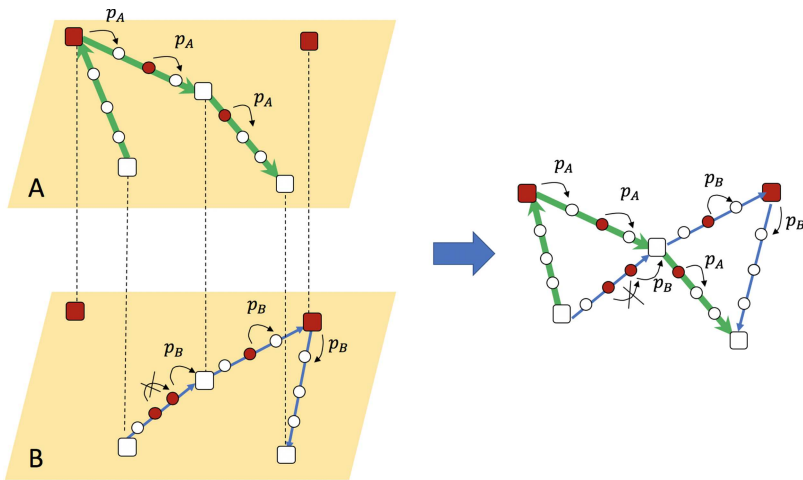


FIG. 1. Illustration of the model. The squares and circles represent the vertices and inner sites at links, respectively. The red (white) color indicates the site is (not) occupied by a particle. On each link, the movements of the particles are subject to the 1-D TASEP transport rule. In the upper layer, every particle hops with probability $p_A = 1$ if its neighbor site in the link direction is vacant. In the lower layer, each particle hops with probability $p_B < 1$. Note that the vertices in the two-layer networks are the same. The overlay of the two networks is shown at the right.

For the segment $u \rightarrow v$, the entry and exit rates are

$$\alpha = \frac{p_{uv}\rho_u}{c}, \quad \beta = p_{uv}(1 - \rho_v). \tag{4}$$

The first equation takes into account the probability that a particle occupying vertex u chooses an outgoing segment $u \rightarrow v$ at random ($1/c$) and successfully moves into the first site of the segment (p_{uv}). The second equation considers the case that a particle occupying the last site of the segment $u \rightarrow v$ moves to the unoccupied vertex v . Inserting Eq. (4) into (3), we have

$$\begin{aligned} \frac{\partial \rho_v}{\partial t} = & \sum_{u \rightarrow v} J_{\text{seg}} \left(p_{uv}, \frac{p_{uv}\rho_u}{c}, p_{uv}(1 - \rho_v) \right) \\ & - \sum_{w \leftarrow v} J_{\text{seg}} \left(p_{vw}, \frac{p_{vw}\rho_v}{c}, p_{vw}(1 - \rho_w) \right). \end{aligned} \tag{5}$$

Employing Eqs. (1) and (2), the above differential equations can be solved numerically. Finally, we obtain the stationary value of the average occupancy for each vertex, based on which, we can further calculate the global current J .

IV. TASEP ON SINGLE-LAYER NETWORKS

In this section, we consider the totally asymmetric simple exclusion process on single-layer networks, where all the segments in the network are the same type, i.e., the hopping probability of particles on each link is a constant p . The situation that $p = 1$ has been fully investigated in Ref. 11. We here address the general case where $0 \leq p \leq 1$.

In the single-layer networks (note that the underlying network considered here is a random regular network), all vertices, as well as all segments, are equivalent. Thus, the global current J is equal to the current on each segment, which can be computed by using Eqs. (1), (2), and (4),

$$J = J_{\text{seg}} = \begin{cases} \frac{p\rho_u}{c} (1 - \frac{\rho_u}{c}), & \rho_u < \frac{c}{c+1}, \\ p \frac{c}{(1+c)^2}, & \rho_u = \frac{c}{c+1}, \\ p\rho_u (1 - \rho_u), & \rho_u > \frac{c}{c+1}. \end{cases} \tag{6}$$

Similarly, the global particle density ρ is equal to the bulk density in each segment, satisfying

$$\rho = \rho_{\text{seg}} = \begin{cases} \frac{\rho_u}{c}, & \rho_u < \frac{c}{c+1}, \\ \rho_u, & \rho_u > \frac{c}{c+1}. \end{cases} \tag{7}$$

When $\rho_u = c/(c + 1)$ (i.e., $\alpha = \beta$), ρ can be any value between ρ_u/c and ρ_u , since the LD and HD zones coexist in each segment, and the interface can be in any position on the segment.⁸ According to Eqs. (6) and (7), we obtain the current-density relation

$$J = \begin{cases} p \frac{c}{(c+1)^2}, & \rho^* < \rho < 1 - \rho^* \\ p\rho(1 - \rho), & \text{otherwise,} \end{cases} \tag{8}$$

where $\rho^* = 1/(c + 1)$ is independent of p .

Figure 2 shows how the global current J changes with the overall particle density ρ for different values of p . It can be seen that

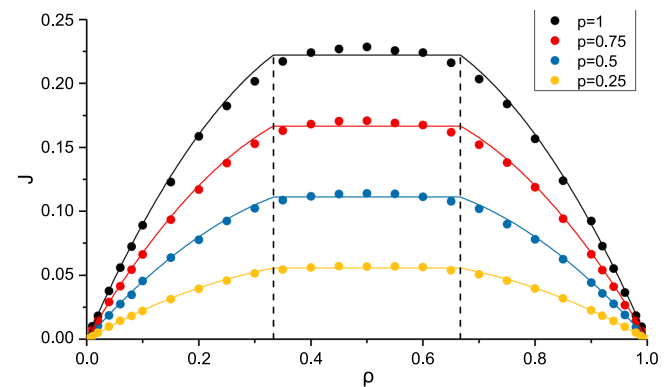


FIG. 2. The global current J as a function of the overall particle density ρ for different values of p . In the simulations (solid circles), the parameters are chosen as $N = 40$, $L = 100$, and $c = 2$. The solid lines correspond to the mean-field predictions. The black, red, blue, and yellow colors represent $p = 1, 0.75, 0.5$, and 0.25 , respectively.

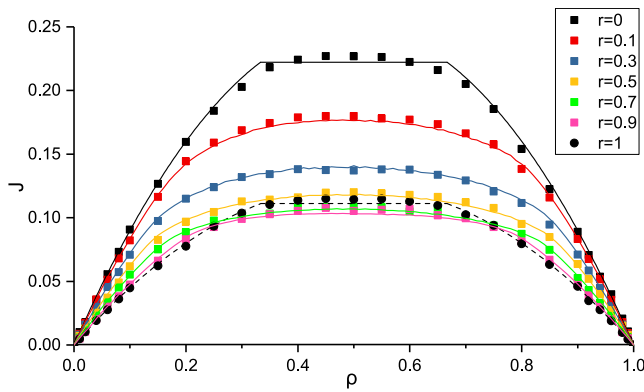


FIG. 3. The global current J as a function of the overall particle density ρ for different values of r , which represents the fraction of the low-speed segments with $p_B = 0.5$. The symbols (squares and circles) are the simulation results; the (dashed) lines are obtained from the numerical solutions of Eq. (5). The parameters are set as $N = 40$, $L = 100$, $c = 2$, and $p_A = 1$.

J is a parabolic function of ρ , which is truncated by a plateau-like region at intermediate values. Correspondingly, the system can be in three different phases as ρ increases: low density, shock phase, and high density (the different phases are separated by the dashed lines in the figure). Furthermore, as p decreases, the global current drops, while the plateau-like region keeps unchanged (i.e., the parameter p cannot affect the phases). The theoretical predictions fit the simulation results perfectly.

V. TASEP ON MULTIPLEX NETWORKS

We then investigate the case $r > 0$ (r is the fraction of segments with hopping probability p_B), in which the underlying network is multiplex. Clearly, for $r = 0$ ($r = 1$), the movements of particles on

all segments are fast (slow). We first study how the parameter r may influence the current-density relation. Figure 3 illustrates the global current J as a function of density ρ for different values of r . For convenience, we choose $p_A = 1$ and $p_B = 0.5$ here. We see that the plateau-like effect disappears since the segments are no longer homogeneous as assumed in Sec. IV. Moreover, as r decreases from 1 to 0, in both low and high density regions, the global traffic flow increases, which adheres to our intuition. While at the intermediate values of ρ , the situation is different: as r decreases, the global current first drops slightly, then rises.

To confirm the above results, we further plot the current J as a function of r for various hopping probability p_B . When the particle density is small ($\rho = 0.2$), J decreases monotonously as r increases [Fig. 4(a)]. It is worth noticing that for small values of p_B , J drops rapidly at first and then decreases gradually in a range of large values of r . This phenomenon indicates that when all particles move fast ($r = 0$), lowering the hopping rate of particles on a fraction of segments may lead to a large decrease in the global traffic flow (like cascading failure process). In contrast, when $r = 1$, all particles move with a smaller probability p_B . In this case, raising the hopping rate of a few segments, however, has limited effects on increasing the global current, due to the constraints from the low-speed segments on the high-speed ones. The similar phenomena can also be observed for large particle densities owing to the particle-hole symmetry [see Fig. 4(c), where $\rho = 0.8$].

Yet for the intermediate values of ρ , the current J is a nonmonotonic function of the parameter r , as shown in Fig. 4(b). It is easy to see that as r increases, J first drops noticeably and then rises slightly as r increases, displaying a concave shape. This result suggests that for large r , lowering (raising) the traveling speed of particles on a small fraction of the segments may lead to a better (worse) performance in the global traffic flow, which is a counterintuitive finding. It reminds us of the classical Braess paradox,³⁵ which states that adding a new road to a road network may possibly degrade its overall performance, like increasing the travel time of each driver. However,

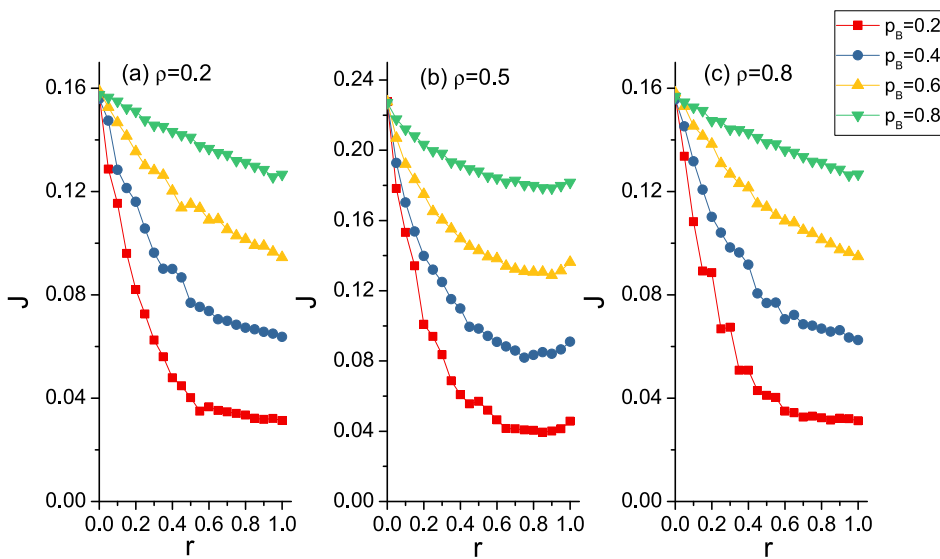


FIG. 4. The global current J changes with the fraction of the low-speed segments for different values of overall particle density: (a) $\rho = 0.2$, (b) $\rho = 0.5$, (c) $\rho = 0.8$. The different symbols (or colors) stand for different values of p_B . The parameters are set as $N = 40$, $L = 100$, $c = 2$, and $p_A = 1$.

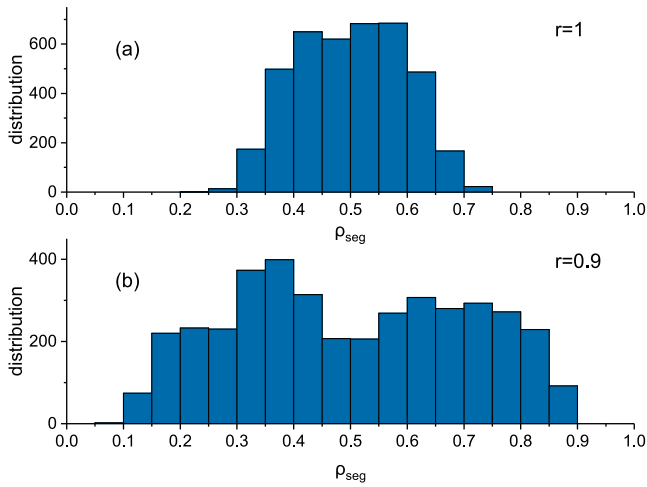


FIG. 5. Distributions of the segment densities for (a) $r = 1$, where all segments have the same hopping probability $p_B = 0.5$ and (b) $r = 0.9$, where 10% of the segments are high-speed links with hopping probability $p_A = 1$. The other parameters are $N = 40$, $L = 100$, $c = 2$, and $\rho = 0.5$. The results are averaged over 50 different realizations.

there are essential differences between the two cases: the Braess paradox is a result from the decisions made by “rational” agents, while in our model, the particles travel at random, and the “paradox” is rooted in the multiplex structure.

To explain it, we analyze how the particles are distributed across the segments in the network. Consider the case where $p_A = 1$,

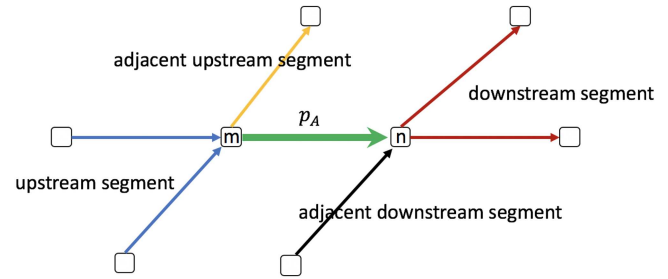


FIG. 6. The classification of the neighbor segments of a segment $m \rightarrow n$ in layer A. The blue (red) links pointing to (leaving from) vertex m (n) are defined as upstream (downstream) segments, and the yellow (black) links leaving from (pointing to) vertex m (n) are defined as adjacent upstream (downstream) segments.

$p_B = 0.5$, and $\rho = 0.5$, we show that, when $r = 1$, the distribution of segment densities (defined as the number of particles on a segment divided by the number of sites L of that segment) is concentrated in the range of $(0.3, 0.7)$ [see Fig. 5(a)]. Decreasing r to 0.9, i.e., 10% of the segments are set to be high-speed links with hopping probability $p_A = 1$, the distribution tends to be bimodal—the number of segments with low and high densities goes up, as shown in Fig. 5(b), which may result in the decrease in the current [referring to Eq. (2)].

To better understand the effects of the high-speed segments on the traffic flow in detail, we classify the neighbor segments of each segment in layer A into four types, as shown in Fig. 6. Suppose $m \rightarrow n$ is a segment from layer A. We define the segments pointing to vertex m as upstream segments, and the segments leaving from

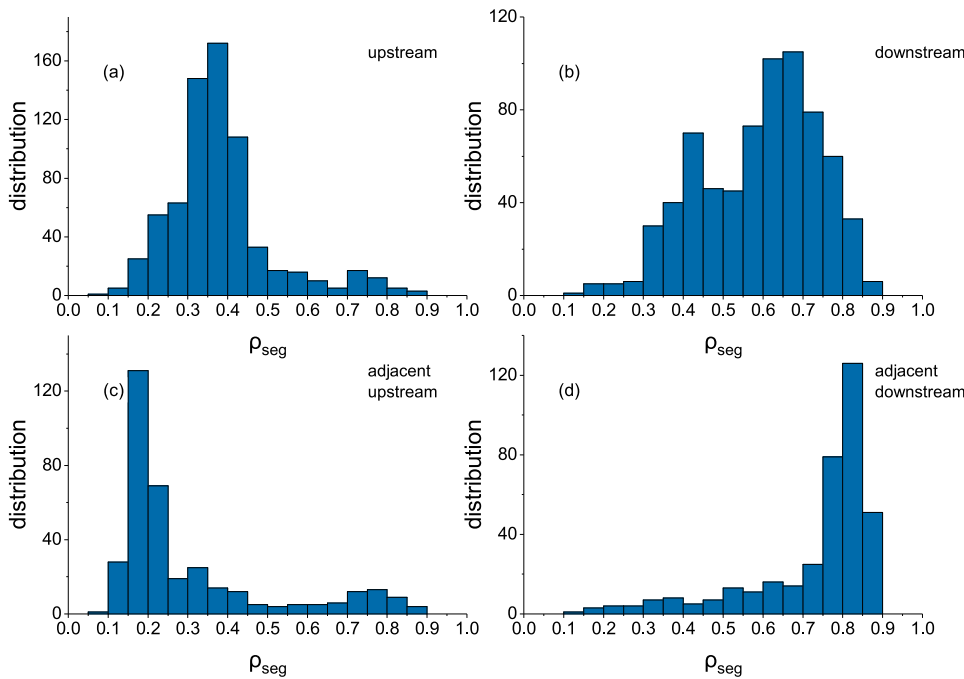


FIG. 7. Distributions of the segment densities for four different types of segments: (a) upstream segments, (b) downstream segments, (c) adjacent upstream segments, (d) adjacent downstream segments. In the simulation, the parameters are $N = 40$, $L = 100$, $c = 2$, $\rho = 0.5$, $p_A = 1$, $p_B = 0.5$, and $r = 0.9$. The results are averaged over 50 different realizations.

vertex n as downstream segments. Moreover, we further define the segments leaving from vertex m (excluding the segment $m \rightarrow n$) as adjacent upstream segments, and the segments pointing to vertex n as adjacent downstream segments.

Figure 7 shows the distributions of the segment densities for the four types of segments. Here, we focus on the influence of the segments in layer A on the segments in layer B (i.e., excluding the segments with $p_A = 1$). We see that, on average, the particle densities on (adjacent) upstream segments are at low levels, while the densities on (adjacent) downstream segments are at high levels. This accounts for the bimodal distribution as observed in Fig. 5(b). The reason that the upstream segments have low densities of particles is straightforward: since the particles on the segments in layer A move with a higher probability, the exit rates [$\sim p_A(1 - \rho_m)$] of the upstream segments increase, yet the entry rates ($\sim p_B \rho_m / c$) of the adjacent upstream segments decrease (due to the decrease in the average occupancy of vertex m). The similar analyses can be applied to the downstream and adjacent downstream segments.

VI. CONCLUSION

In summary, we have studied the TASEP on multiplex networks where the segments (links) are classified into two types according to the hopping rate of particles on them. The hopping rate of particles on one type of segments is larger than that on the other type of segments. The main conclusion is that, in the low and high density regions, the global current drops monotonously as the fraction r of the low-speed segments increases. Nevertheless, at the intermediate values of particle density, as the number of high-speed segments increases, the global current drops slightly in a range of large values of r . We have shown that the high-speed segments, on one hand, may cause the particle densities of their downstream segments to increase (since more particles flow in per unit time), and on the other hand, may cause the particle densities of their upstream segments to decrease (since more particles flow out per unit time), resulting in a bimodal distribution of the segment densities. This kind of particle distribution accounts for the counterintuitive phenomenon (note that whether the particle density of a segment is too low or too high, the current on it is small). It is worth noticing that our multiplex network model is based on the directed random regular network, which could be extended to more complicated cases. We found that, for example, the same phenomenon could also be observed in BA networks, although the result is not as obvious as shown in the case of regular networks. The results presented here may provide some interesting insights in reality, such as transportation infrastructure construction.

ACKNOWLEDGMENTS

This work was partially supported by the National Natural Science Foundation of China (NNSFC) under Grant Nos. 11605154 and 61771430 and the Zhejiang Provincial Natural Science Foundation of China under Grant No. LY20F030018.

REFERENCES

- Z. Zheng, Z. Huang, F. Zhang, and P. Wang, "Understanding coupling dynamics of public transportation networks," *EPJ Data Sci.* **7**, 23 (2018).
- Z. Ruan, C. Song, X. Yang, G. Shen, and Z. Liu, "Empirical analysis of urban road traffic network: A case study in Hangzhou city, China," *Physica A* **527**, 121287 (2019).
- G. Zeng *et al.*, "Switch between critical percolation modes in city traffic dynamics," *Proc. Natl. Acad. Sci. U.S.A.* **116**, 23 (2019).
- D. Brockmann, L. Hufnagell, and T. Geisel, "The scaling laws of human travel," *Nature* **439**, 462 (2006).
- M. C. González, C. A. Hidalgo, and A.-L. Barabási, "Understanding individual human mobility patterns," *Nature* **453**, 779 (2008).
- Z. Ruan, M. Tang, C. Gu, and J. Xu, "Epidemic spreading between two coupled subpopulations with inner structures," *Chaos* **27**, 103104 (2017).
- Z. Ruan, P. Hui, H. Lin, and Z. Liu, "Risks of an epidemic in a two-layered railway-local area traveling network," *Eur. Phys. J. B* **86**, 13 (2013).
- B. Derrida, E. Domany, and D. Mukamel, "An exact solution of a one-dimensional asymmetric exclusion model with open boundaries," *J. Stat. Phys.* **69**, 667 (1992).
- B. Derrida, "An exactly soluble non-equilibrium system: The asymmetric simple exclusion process," *Phys. Rep.* **301**, 65 (1998).
- J. T. MacDonald, J. H. Gibbs, and A. C. Pipkin, "Kinetics of biopolymerization on nucleic acid templates," *Biopolymers* **6**, 1 (1968).
- I. Neri, N. Kern, and A. Parmeggiani, "Totally asymmetric simple exclusion process on networks," *Phys. Rev. Lett.* **107**, 068702 (2011).
- N. Bunzarova, N. Pesheva, and J. Brankov, "Asymmetric simple exclusion process on chains with a shortcut," *Phys. Rev. E* **89**, 032125 (2014).
- Y. Yuan, R. Jiang, R. Wang, M. Hu, and Q. Wu, "Totally asymmetric simple exclusion process with a shortcut," *J. Phys. A* **40**, 12351 (2007).
- D. Huang, "Phase diagram of a traffic roundabout," *Physica A* **383**, 603 (2007).
- Z.-P. Cai *et al.*, "Asymmetric coupling in multi-channel simple exclusion processes," *J. Stat. Mech.* **2008**, P07016 (2008).
- N. Bunzarova, N. Pesheva, and J. Brankov, "On the appearance of traffic jams in a long chain with a shortcut in the bulk," *Physica A* **438**, 645 (2015).
- C. Arita, M. F. Fouladivand, and L. Santen, "Signal optimization in urban transport: A totally asymmetric simple exclusion process with traffic lights," *Phys. Rev. E* **95**, 032108 (2017).
- Y. Wang, R. Jiang, and Q. Wu, "Dynamics in phase transitions of TASEP coupled with multi-lane SEPs," *Nonlinear Dyn.* **88**, 1631 (2017).
- Y. Wang *et al.*, "Dynamics in multi-lane TASEPs coupled with asymmetric lane-changing rates," *Nonlinear Dyn.* **88**, 2051 (2017).
- Y. Baek, M. Ha, and H. Jeong, "Effects of junctional correlations in the totally asymmetric simple exclusion process on random regular networks," *Phys. Rev. E* **90**, 062111 (2014).
- P. Mottishaw, B. Waclaw, and M. R. Evans, "An exclusion process on a tree with constant aggregate hopping rate," *J. Phys. A* **46**, 405003 (2013).
- S. Bittihn and A. Schadschneider, "Braess paradox in a network of totally asymmetric exclusion processes," *Phys. Rev. E* **94**, 062312 (2016).
- S. Boccaletti *et al.*, "The structure and dynamics of multilayer networks," *Phys. Rep.* **544**, 1 (2014).
- M. Kivelä *et al.*, "Multilayer networks," *J. Complex Netw.* **2**, 203 (2014).
- C. D. Brummitt, K. M. Lee, and K. I. Goh, "Multiplexity-facilitated cascades in networks," *Phys. Rev. E* **85**, 045102 (2012).
- M. De Domenico, V. Nicosia, A. Arenas, and V. Latora, "Structural reducibility of multilayer networks," *Nat. Commun.* **6**, 6864 (2015).
- A. Cardillo *et al.*, "Modeling the multi-layer nature of the European air transport network: Resilience and passengers re-scheduling under random failures," *Eur. Phys. J. Spec. Top.* **215**, 23 (2013).
- Z. Ruan, C. Wang, P. Hui, and Z. Liu, "Integrated travel network model for studying epidemics: Interplay between journeys and epidemic," *Sci. Rep.* **5**, 11401 (2015).

²⁹Z. Ruan, M. Tang, and Z. Liu, "Epidemic spreading with information-driven vaccination," *Phys. Rev. E* **86**, 036117 (2012).

³⁰Z. Ruan, J. Wang, Q. Xuan, C. Fu, and G. Chen, "Information filtering by smart nodes in random networks," *Phys. Rev. E* **98**, 022308 (2018).

³¹M. Dickison, S. Havlin, and H. E. Stanley, "Epidemics on interconnected networks," *Phys. Rev. E* **85**, 066109 (2012).

³²A. Saumell-Mendiola, M. A. Serrano, and M. Boguna, "Epidemic spreading on interconnected networks," *Phys. Rev. E* **86**, 026106 (2012).

³³C. Granell, S. Gomez, and A. Arenas, "Dynamical interplay between awareness and epidemic spreading in multiplex networks," *Phys. Rev. Lett.* **111**, 128701 (2013).

³⁴M. E. Fouladvand, S. Chaaboki, and M. Saalehi, "Characteristics of the asymmetric simple exclusion process in the presence of quenched spatial disorder," *Phys. Rev. E* **75**, 011127 (2007).

³⁵E. I. PasShari and L. Principio, "Braess' paradox: Some new insights," *Transp. Res. A* **31**, 265 (1997).